

**Two-dimensional Ising transition through a technique from two-state opinion-dynamics models**

Serge Galam\*

*CEVIPOF-Center for Political Research, Sciences Po and CNRS, 98 rue de l'Université, 75007 Paris, France*

André C. R. Martins†

*GRIFE-EACH-Universidade de São Paulo, Rua Arlindo Btito, 1000, 03828-000, São Paulo, Brazil*

(Received 12 March 2013; revised manuscript received 27 May 2014; published 6 January 2015)

The Ising ferromagnetic model on a square lattice is revisited using the Galam unifying frame (GUF), set to investigate two-state opinion-dynamics models. When combined with Metropolis dynamics, an unexpected intermediate “dis/order” regime is found with the coexistence of two attractors associated, respectively, to an ordered and a disordered phases. The basin of attraction of initial conditions for the disordered phase attractor starts from zero size at a first critical temperature  $T_{c1}$  to embody the total landscape of initial conditions at a second critical temperature  $T_{c2}$ , with  $T_{c1} \approx 1.59$  and  $T_{c2} \approx 2.11$  in  $J/k_B$  units. It appears that  $T_{c2}$  is close to the Onsager result  $T_c \approx 2.27$ . The transition, which is first-order-like, exhibits a vertical jump to the disorder phase at  $T_{c2}$ , reminiscent of the rather abrupt vanishing of the corresponding Onsager second-order transition. However, using Glauber dynamics combined with GUF does not yield the intermediate phase and instead the expected classical mean-field transition is recovered at  $T_c \approx 3.09$ . Accordingly, although the “dis/order” regime produced by the GUF-Metropolis combination is not physical, it is an intriguing result to be understood. In particular the fact that Glauber and Metropolis dynamics yield so different results using GUF needs an explanation. The possibility of extending GUF to larger clusters is discussed.

DOI: [10.1103/PhysRevE.91.012108](https://doi.org/10.1103/PhysRevE.91.012108)

PACS number(s): 75.10.Hk, 64.60.De

**I. INTRODUCTION**

The Ising model is a seminal model of statistical physics, which has inspired thousands of scientific papers [1,2]. In particular, the two-dimensional nearest-neighbor square lattice ferromagnetic Ising model is a cornerstone to the understanding of collective phenomena being the unique case to exhibit a second-order phase transition with an exact analytical solution [3]. All its properties are considered to be known. However, investigating the two-dimensional nearest-neighbor ferromagnetic Ising model through a technique from two-state opinion-dynamics models, is found to raise intriguing questions, yet in lack of an explanation.

Indeed, applying Galam unifying frame (GUF), set to embody most discrete two-state models of opinion dynamics [4], combined with Metropolis dynamics for the probability of a single spin flip [5,6], reveals an unexpected twofold order-disorder Ising transition. The transition is no longer at once from the ordered state into the disordered state but instead goes through an intermediate phase denoted “dis/order” phase, for which two attractors exist, each one being associated to a different basin of attraction of initial conditions. Their respective sizes are a function of the temperature.

The basin of initial conditions to the disordered phase starts from zero size at a first critical temperature  $T_{c1} \approx 1.59$  to end up embodying the total landscape of initial conditions at a second critical temperature  $T_{c2} \approx 2.11$ . Temperature values are given in  $J/k_B$  units where  $J$  is the positive coupling constant and  $k_B$  the Boltzmann constant. To make the presentation lighter from now on we take  $J/k_B = 1$ .

For the Ising system, noting  $p$  the proportion of spins in state  $+1$  and  $(1 - p)$  the proportion of spins in state  $-1$ , three different regimes are obtained for the dynamics as a function of temperature.

(i) Starting at  $T = 0$  the phase diagram contains two attractors,  $p_- = 0$  and  $p_+ = 1$ , with a separator,  $p_c = \frac{1}{2}$ . Increasing temperature moves the two attractors toward the separator with  $p_- > 0$  and  $p_+ < 1$ .

(ii) Then, at a temperature  $T_{c1}$  the separator  $p_c = \frac{1}{2}$  turns to an attractor as expected for the continuous order-disorder Ising transition. However, while in the classical scheme, the change of status from separator to attractor is turned on by the simultaneous merging of the two attractors  $p_-$  and  $p_+$  at  $p_c = \frac{1}{2}$ , here an opposite process occurs. Two new symmetrical separators,  $p_{c-} < \frac{1}{2}$  and  $p_{c+} = 1 - p_{c-} > \frac{1}{2}$ , are expelled from  $p_c = \frac{1}{2}$ , when its status shifts from separator to attractor. That is an unexpected process. As shown in Fig. 2, three attractors and two separators are found in the range  $T_{c1} < T < T_{c2}$  where only two attractors and one separator are expected.

(iii) Keeping on increasing the temperature, on each side of the attractor  $p_c = \frac{1}{2}$ , the attractor  $p_-$  ( $p_+$ ) and the new separator  $p_{c-}$  ( $p_{c+}$ ) move toward each other to eventually coalesce at a second critical temperature  $T_{c2}$  and then disappear. In the range  $T > T_{c2}$  only the attractor  $p_c = \frac{1}{2}$  exists and corresponds to the disordered phase. In addition, it happens that  $T_{c2} \approx 2.11$  is very close to the Onsager exact result  $T_c \approx 2.27$ . Moreover, the transition being first-order-like, it exhibits a vertical jump to the disorder phase at  $T_{c2}$ , which is reminiscent of the rather abrupt vanishing of the corresponding Onsager magnetization at the second-order transition.

However, and in contrast, performing the same calculations as above using Glauber dynamics combined to GUF instead of Metropolis dynamics, restores the expected phase diagram

\* [serge.galam@sciencespo.fr](mailto:serge.galam@sciencespo.fr)† [amartins@usp.br](mailto:amartins@usp.br)

with one continuous transition from the ordered phase into the disordered phase at  $T_c \approx 3.09$  against  $T_c = 4$  for the classical mean-field counterpart. It is worth noting that the formula obtained for  $T_c \approx 3.09$  using Glauber dynamics is identical to the one obtained by Mamada and Takamo [7], although the associated polynomial equations have different coefficients.

Accordingly, although the “dis/order” regime produced by the GUF-Metropolis combination is not physical, its finding is an intriguing result to be understood theoretically. Moreover, the fact that Glauber and Metropolis dynamics yield such different results using GUF needs an explanation. The possibility of extending GUF to larger clusters is also briefly discussed.

## II. WHAT IS GUF?

Among the numerous applications of the Ising model, a large number has been devoted to study opinion dynamics within the field of sociophysics [8], where two opinions are competing among agents experiencing some local interactions. However, up to today there exist no established first principles that we are aware of to settle the selection of the local update rule, which monitors the dynamics of opinion changes among agents, making each peculiar *ad hoc* choice the seed of a “new” model. Accordingly a large number of models have been proposed in the literature leading to some confusion on identifying which actual social mechanisms are behind the making of a collective opinion [9–14].

To address the above difficulty, a unifying frame was shown to embody most of the discrete binary models [4], showing that the actual update rule is not the relevant feature of those models. It thus happens that many different settings of interactions among agents leads to the same phase diagram. The unifying frame basic principle is usually referred to in the literature as the Galam unifying frame or Galam model [15–19]. Another proposal of opinion dynamics first principles was also suggested recently [20].

Given a number of interacting agents, GUF enumerates all possible corresponding groupings of agents. Then an update of individual states is applied for each group according to the specificity of the interactions. Then all agents are randomly reshuffled to obtain a new distribution within the same setting of local groups. The process is repeated until an equilibrium state is obtained. A general sequential probabilistic frame is thus built from which a phase diagram can be constructed.

For two-state variables two phases are found, one where the collective opinion is broken along one opinion, thus stabilizing it as the majority, which can eventually coexist with a minority (ordered phase), and another phase with a balanced coexistence of both opinions (disordered phase). Two different regimes, monotonic and dampened oscillatory, are found for the coexistence phase. At the phase transition, local probabilities conserve the density of opinions and reproduce the collective dynamics of the Voter model.

More precisely, consider a population of  $N$  two-state agents ( $S_i = \pm 1$ ) with  $i = 1, \dots, N$  and some local update rule that involves a number  $r$  of agents. Given at time  $t$  a proportion  $p(t)$  of agents in state  $S_i = +1$  and  $[1 - p(t)]$  in state  $S_i = -1$  the dynamics is implemented in three successive steps:

- (i) all agents are randomly distributed in distinct groups of size  $r$ ,
  - (ii) the update rule is applied separately within each group,
  - (iii) all agents are reshuffled,
- which are then iterated a certain number of times.

To implement above steps all possible configurations of agents in a group of size  $r$  are enumerated. Within each group the number  $v$  of agents in state  $S_i = +1$  can vary from  $v = 0$  up to  $v = r$ . For each value  $v$  there exist  $C_r^v \equiv \frac{r!}{v!(r-v)!}$  different configurations denoted, respectively,  $t$  with  $t = 1, \dots, C_r^v$ .

For each configuration  $t$  the specific update rule denoted  $T_{v_t \rightarrow w_t}^r$  yields a number  $w_t$  of agents in state  $S_i = +1$  with  $0 \leq w_t \leq r$ . Therefore, the probability to have a group of  $r$  agents with  $v$  agents in state  $S_i = +1$  and  $(r - v)$  agents in state  $S_i = -1$  ending with  $w \equiv \sum_{t=1}^{C_r^v} w_t$  agents in state  $S_i = +1$  and  $(r - w)$  agents in state  $S_i = -1$  writes,

$$\sum_{t=1}^{C_r^v} p(t)^v [1 - p(t)]^{r-v} T_{v_t \rightarrow w_t}^r. \quad (1)$$

Summing from  $v = 0$  up to  $v = r$  yields the new proportion  $p(t + 1)$  of agents in state  $S_i = +1$  starting from  $p(t)$  after one cycle of update with,

$$p(t + 1) = \sum_{v=0}^r p(t)^v [1 - p(t)]^{r-v} \sum_{t=1}^{C_r^v} T_{v_t \rightarrow w_t}^r \frac{w_t}{r}, \quad (2)$$

where  $\frac{w_t}{r}$  accounts for the contribution to the  $S_i = +1$  state from the updated group.

In addition, the topology of the network may involve groups of different sizes  $r$  for the update. Denoting  $a_r$  the proportion of groups of size  $r$  and  $L$  the size of the larger group involved, we have the constraint,

$$\sum_{r=1}^L a_r = 1, \quad (3)$$

which allows us to generalize Eq. (2) to obtain,

$$p(t + 1) = \sum_{r=1}^L a_r \sum_{v=0}^r p(t)^v [1 - p(t)]^{r-v} \sum_{t=1}^{C_r^v} T_{v_t \rightarrow w_t}^r \frac{w_t}{r}, \quad (4)$$

However, in case  $T_{v_t \rightarrow w_t}^r$  is a probability distribution  $T_{v_t \rightarrow w_{t,z}}^r$  yielding  $Z$  different values  $w_{t,z}$  ( $0 \leq w_{t,z} \leq r$ ), Eq. (4) becomes

$$p(t + 1) = \sum_{r=1}^L a_r \sum_{v=0}^r p(t)^v [1 - p(t)]^{r-v} \times \sum_{t=1}^{C_r^v} \sum_{z=1}^Z T_{v_t \rightarrow w_{t,z}}^r \frac{w_{t,z}}{r}, \quad (5)$$

with  $\sum_{z=1}^Z T_{v_t \rightarrow w_{t,z}}^r = 1$ , which is the general GUF update equation.

After the first update, items (i) and (ii), agents are reshuffled, item (iii). Then above scheme is repeated redistributing the agents randomly among the various groups to be updated again. A new proportion of  $p(t + 2)$  of agents in state  $S_i = +1$  is thus obtained from  $p(t + 1)$  using Eq. (5). The same process

is iterated a number  $k$  of times till a fixed point is reached where no change occurs with  $p(t+k) = p(t+k+1)$ . Indeed, to build the complete flow diagram of the dynamics, the fixed point equation  $p(t) = p(t)$  is solved to extract the separators and attractors of the dynamics.

Using Eq. (4) allows us to recover all existing discrete two-state models [11,21–29], which are shown to depart from each other only in the setting of their local rule  $T_{v \rightarrow w}^r$ , which nevertheless leads to the same attractors. Accordingly, one cannot conclude on the validity of the psychosociological assumptions used in a model as a function of the validity of its results since what matters is the symmetry of the update rule and not the corresponding values of the local probabilities of shift.

At this stage it is worth emphasizing that GUF requires neither the use of thermodynamics nor the knowledge of a Hamiltonian. Only the update rule is required making GUF a robust scheme to implement to any kind of problem. Such a feature prompts us to apply it to the classical 2D Ising model.

### III. APPLYING GUF TO THE ISING MODEL

#### A. The 2D Ising model

With no external field, the Hamiltonian for the square lattice ferromagnetic Ising system is given by

$$H = -\frac{J}{2} \sum_{[ij]} \sigma_i \sigma_j, \quad (6)$$

where  $[ij]$  a sum over all nearest neighbors  $i$  and  $j$  and  $\sigma_i = \pm 1$ . The associated magnetization is  $M = \frac{1}{N} \sum_i \sigma_i = 2p - 1$ , where  $N$  is the total number of spins.

The problem has been solved exactly with  $T_c = 2/\text{arcsinh}(1) \approx 2.27$ . In contrast, the classical mean-field approach yields  $T_c = 4$ .

However, in higher dimensions or with an external field, Monte Carlo (MC) simulations are required. They are implemented using a dynamics that respects detailed balance. The most common ones are the Glauber and Metropolis dynamics [5,6]. In the Glauber dynamics, all spins are investigated in a sequential manner for each MC step. Given a spin  $\sigma_i$  in a configuration  $\mu_i$  with energy  $E_{\mu_i}$ , the flip  $\sigma_i \rightarrow -\sigma_i$  creates the new configuration  $\eta_i$  with energy  $E_{\eta_i} = -E_{\mu_i}$ . The actual flip is implemented with the probability

$$G_{\mu_i \rightarrow \eta_i} = \frac{1}{1 + \exp(-2E_{\mu_i}/k_B T)}. \quad (7)$$

In the Metropolis scheme, the spin is selected randomly and a MC step corresponds to  $N$  updates. The flip probability to the new configuration is given by

$$M_{\mu_i \rightarrow \eta_i} = \min\{1, \exp[2E_{\mu_i}/k_B T]\}. \quad (8)$$

#### B. GUF update equation

Applying GUF to the classical nearest-neighbor ferromagnetic Ising model on a square lattice requires to use only groups of size  $r = 5$  since each spin update involves its four nearest neighbors. Therefore, the associated polynomial development

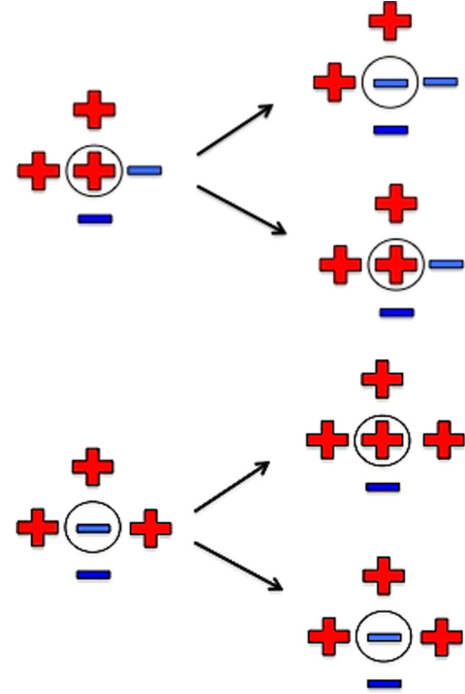


FIG. 1. (Color online) Configurations with three spins (+) and two spins (-). The associated  $C_5^3 = 10$  configurations split in two subgroups with respect to the update, one with six configurations  $t_+ \equiv t_1, \dots, t_6$  having a central spin (+) (upper left part) and one with four configurations  $t_- \equiv t_7, \dots, t_{10}$  having a central spin (-) (lower left part). In each case, right side shows the corresponding configurations with the central spin shifted (upper part) and the central spin unchanged (lower part).

for the update function is of degree 5 yielding for Eq. (5),

$$p(t+1) = \sum_{v=0}^5 p(t)^v [1 - p(t)]^{5-v} \sum_{t=1}^{C_5^v} \sum_{w_i=0}^5 T_{v_i \rightarrow w_i}^5 \frac{w_i}{5}, \quad (9)$$

where going from time  $t$  to time  $t+1$  corresponds to one MC step. However, here, only the central spin is updated with a probability given by either Glauber or Metropolis schemes ( $Z = 2$ ) keeping the other four spins unchanged.

For instance, in the case  $r = 5$  and  $v = 3$  the associated  $C_5^3 = 10$  configurations split in two subgroups with respect to the update, one with six configurations  $t_+ \equiv t_1, \dots, t_6$  having a central spin (+) (upper part of Fig. 1) and one with four configurations  $t_- \equiv t_7, \dots, t_{10}$  having a central spin (-) (lower part of Fig. 1).

When the central spin is flipped the associated energies changes are, respectively,  $E_{\mu} = 0 \rightarrow E_{\eta} = 0$  (upper part) and  $E_{\mu} = 2J \rightarrow E_{\eta} = -2J$  (lower part). Writing  $b \equiv e^{-4/T}$  and noticing that  $w_{t_{+1}} = 2$  and  $w_{t_{+2}} = 3$ , the Glauber associated transition rates are  $T_{3 \rightarrow 2}^5 = T_{3 \rightarrow 3}^5 = 1/2$  for both  $+ \rightarrow -$  and  $+ \rightarrow +$  (upper part). For the lower part  $w_{t_{-1}} = 4$  and  $w_{t_{-2}} = 3$   $T_{3 \rightarrow 4}^5 = \frac{1}{1+b}$  for  $- \rightarrow +$  and  $T_{3 \rightarrow 3}^5 = \frac{b}{1+b}$  for  $- \rightarrow -$ .

For the same cases of Fig. 1 using Metropolis the upper part leads to  $T_{3 \rightarrow 2}^5 = 1$  for  $+ \rightarrow -$  and  $T_{3 \rightarrow 3}^5 = 0$  for  $+ \rightarrow +$ . For the lower part  $T_{3 \rightarrow 4}^5 = 1$  for  $- \rightarrow +$  and  $T_{3 \rightarrow 3}^5 = 0$  for  $- \rightarrow -$ . Accordingly, rescaling with the respective values of  $w_i/5$ , Glauber contributions from the  $r = 5$  and  $v = 3$  to the  $\sigma_i = +1$

proportion are  $6 \times (\frac{1}{2} \times \frac{2}{5} + \frac{1}{2} \times \frac{3}{5}) + 4 \times (\frac{1}{1+b} \times \frac{4}{5} + \frac{b}{1+b} \times \frac{3}{5})$ , yielding

$$\frac{31 + 27b}{5(1+b)} p^3 (1-p)^2, \quad (10)$$

Similarly, Metropolis yields  $6 \times (1 \times \frac{2}{5} + 0 \times \frac{3}{5}) + 4 \times (1 \times \frac{4}{5} + 0 \times \frac{3}{5})$ , with

$$\frac{28}{5} p^3 (1-p)^2. \quad (11)$$

Repeating above calculations for all values of  $v$  and  $w$  from 0 to 5 and using the up-down symmetry yields for Eq. (9) leads for Metropolis,

$$p_M = \frac{1}{5} [(5-b^2)p^5 + (21-4b)p^4(1-p) + 28p^3(1-p)^2 + 22p^2(1-p)^3 + 4(1+b)p(1-p)^4 + b^2(1-p)^5], \quad (12)$$

while Glauber produces,

$$p_G = \frac{1}{5} \left[ \frac{5+4b^2}{1+b^2} p^5 + \left( \frac{5+4b^2}{1+b^2} + \frac{16+12b}{1+b} \right) p^4(1-p) + p^3(1-p)^2 \frac{31+27b}{1+b} + p^2(1-p)^3 \left( \frac{19+23b}{1+b} \right) + \left( \frac{20+21b^2}{1+b^2} - \frac{16+12b}{1+b} \right) p(1-p)^4 + \frac{b^2}{1+b^2} (1-p)^5 \right]. \quad (13)$$

While Eq. (13) seems to be more complicated than Eq. (12), expanding it in powers of  $p$  exhibits a reduction of the polynomial degree from 5 down to 3, with

$$p_G = \frac{(-2p^3+3p^2)(1-b)^3 + 4p(1+2b+b^3) + b^2(1+b)}{5(1+b)(1+b^2)}, \quad (14)$$

which is not the case for Metropolis.

#### IV. UNCOVERING A TWOFOLD TRANSITION

To investigate the dynamics and phase transitions produced by Eqs. (12) and (14) we need to solve the fixed-point equation  $p(t+1) = p(t)$  for each case. The attractors correspond to the equilibrium states while the separator determines the flow direction when implementing the dynamical update.

##### A. GUF-Metropolis

From  $p_M = p$  we get always the solution  $p_c = 1/2$  with 3 different regimes. One with  $p_c = 1/2$  being the unique attractor. The second and third ones have, respectively, two and four symmetrical solutions beyond and below  $p = 1/2$  as shown in Fig. 2. In the second case  $p_c = 1/2$  is a separator

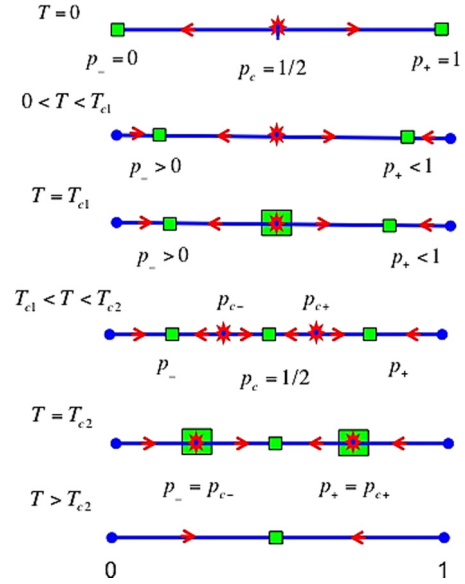


FIG. 2. (Color online) Landscape of the attractors and separators as a function of temperature. The first top corresponds to  $T = 0$  with two attractors  $p_-=0$ ,  $p_+=1$ , and a separator  $p_c = 1/2$ . Second from top corresponds to  $0 \leq T < T_{c1} \approx 1.59$ : same as before with  $p_- \geq 0$  and  $p_+ \leq 1$ . Third from top: at  $T = T_{c1}$  the separator is about to turn into an attractor giving rise to two symmetrical moving separators on each side. Third from bottom: for  $T_{c1} < T < T_{c2}$  three attractors  $p_-$ ,  $p_+$ ,  $p_c$  separated by two the separators  $p_{c-}$ ,  $p_{c+}$ . Second from bottom: at  $T = T_{c2}$  the two separators  $p_{c-}$  and  $p_{c+}$  coalesce with the two attractors  $p_-$ ,  $p_+$  to suppress them. Bottom: only one attractor at  $p_c = 1/2$  for  $T > T_{c2} \approx 2.11$ , which is close to the exact result 2.27.

while it is an attractor in the third case. More precisely, above

$$b_{c2} = \frac{1}{5} \left[ 1 - 16 \left( \frac{2}{15\sqrt{249} - 27} \right)^{\frac{1}{3}} + \left( \frac{2}{3} \right)^{\frac{2}{3}} (5\sqrt{249} - 9)^{\frac{1}{3}} \right] \approx 0.150, \quad (15)$$

we observe only the zero-magnetization solution  $p = 1/2$ . However, below  $b_{c2}$ , in the region defined by  $0 \leq b \leq b_{c1}$  with

$$b_{c1} = \frac{1}{5}(\sqrt{41} - 6) \approx 0.081, \quad (16)$$

we have two solutions for  $p$  given by

$$p_{\pm} = \frac{1}{2C} [C \pm \sqrt{C^2 - 4C(D-E)}], \quad (17)$$

where  $C \equiv (2b^2 - 8b + 6)$ ,  $D \equiv (3b^2 - 4b + 1)$  and  $E \equiv \sqrt{5b^4 - 8b^3 + 10b^2 - 8b + 1}$ . These solutions are attractors. They start from the values  $p_- = 0$  and  $p_+ = 1$  at  $b = 0$  and move toward  $p_c = 1/2$ , which behaves as a separator. However, they do not reach the zero magnetization as  $b \rightarrow b_{c2}$ . Instead, they meet another pair of solutions,

$$p_{c\pm} = \frac{1}{2C} [C \pm \sqrt{C^2 - 4C(D+E)}], \quad (18)$$

which exist only in the interval

$$b_{c1} \leq b \leq b_{c2}. \quad (19)$$

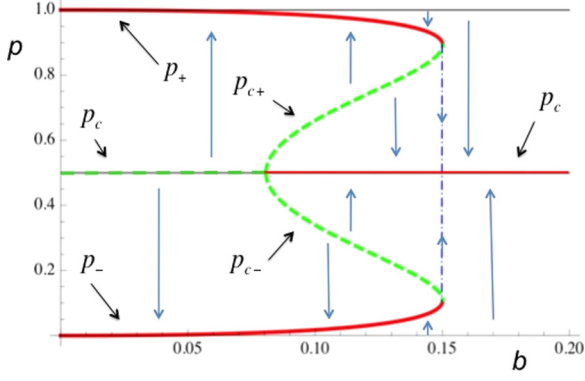


FIG. 3. (Color online) The variation of all the five GUF fixed points as a function of  $b = \exp(-4/T)$  using Metropolis dynamics. The arrows show the flow direction while iterating the local updates. Dark solid lines correspond to attractors, i.e.,  $p_+$ ,  $p_-$  and  $p_c$  for  $b \geq b_{c1}$ . Dashed lines are separators, i.e.,  $p_{c+}$ ,  $p_{c-}$  and  $p_c$  for  $b < b_{c1}$ .

As soon as those two solutions  $p_{c\pm}$  appear, they behave as separators and move toward  $p_c = 1/2$ , which turns at once to an attractor. The values  $b_{c1}$  and  $b_{c2}$  yield the critical temperatures of  $T_{c1} \approx 1.59$  and  $T_{c2} \approx 2.11$  using  $T \equiv -4/\ln b$ . In addition, the fact that for  $b < b_{c2}$ ,  $p_c = 1/2$  is no longer the only solution, could be interpreted as the signature of the actual phase transition occurring at  $T_{c2}$ . This hypothesis provides a much better estimate for the critical temperature than that of mean-field theory, since the correct value is  $T_c \approx 2.27$ . Notice that  $T_{c1} \approx 1.59$  had been previously observed for another attempt of estimating the critical temperature in the context of the GUF framework [30], however missing the existence of  $T_{c2}$ .

The series of diagrams of Fig. 2 shows the moving landscape of attractors and separators as a function of varying the temperature. Two attractors  $p_- = 0$  and  $p_+ = 1$  with a separator  $p_c = 1/2$  are found at  $T = 0$  as expected. Increasing temperature the two attractors move toward the separator with  $p_- > 0$  and  $p_+ < 1$  also as expected. However, at a temperature  $T_{c1} \approx 1.59$  the separator turns to an attractor  $p_c = 1/2$  with the simultaneous appearance of two new symmetrical separators  $p_{c-} < 1/2$  and  $p_{c+} = 1 - p_{c-} > 1/2$ . That is an unexpected result.

Increasing still the temperature, on each side of the attractor  $p_c = 1/2$ , the attractor and the new separator move toward each other to eventually coalesce at  $T_{c1} \approx 2.11$  and then disappear. At  $T > T_{c2}$  only the attractor  $p_c = 1/2$  exists.

Figure 3 shows the variation of all five fixed points as a function of  $b = \exp^{-4/T}$ . The arrows show the flow direction while iterating the local updates. Dark solid lines correspond to attractors, i.e.,  $p_+$ ,  $p_-$  and  $p_c$  for  $b \geq b_{c1}$ . Dashed lines are separators, i.e.,  $p_{c+}$ ,  $p_{c-}$  and  $p_c$  for  $b < b_{c1}$ .

Figures 4 and 5 show the two kinds of dynamics obtained to describe the Metropolis-driven GUF Ising transition. In the first case, Fig. 4 shows the known twofold regimes typical of the Ising transition. At  $b = 0.05 < b_{c1}$  all initial configurations end up at an ordered phase with either a positive ( $p_0 > 0.50$ ) or negative ( $p_0 < 0.50$ ) magnetization, while for  $b = 0.16 > b_{c2}$  all initial configurations end up at the disordered phase with zero magnetization.

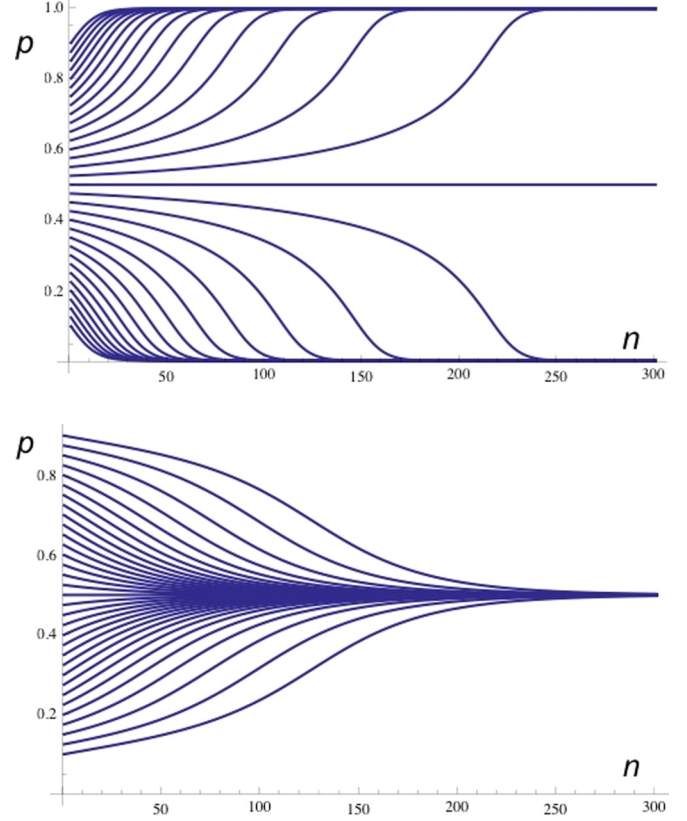


FIG. 4. (Color online) Variation of  $p$  under 300 successive iterations of update rule  $p_G$  using Eq. (12) for initial condition  $p_0 = 0.10 + n \cdot 0.025$  with  $n = 0, 1, 2, \dots, 32$ . Upper part exhibits the dynamics to the ordered phase at temperature  $b = 0.05 < b_{c1}$ . Any initial condition leads to the same nonzero value of the magnetization:  $p_0 > 1/2$  ( $p_0 < 1/2$ )  $\rightarrow$  positive (negative) magnetization. At contrast, in lower part at  $b = 0.16 > b_{c2}$  any initial condition leads to zero magnetization. Both cases correspond to the usual ordered and disordered Ising phases. The number of iterations are labeled along the abscise.

However, the second case exhibits an unexpected dynamics as shown in Fig. 5. At  $b = 0.10$  and  $b = 0.13$ , the equilibrium state at a fixed temperature depends on the initial conditions. Depending on  $p_0$ , two possible states are reached, one with a nonzero magnetization and one with zero magnetization.

## B. GUF-Glauber

We now repeat the above calculations using the Glauber scheme [Eq. (7)] instead of Metropolis [Eq. (8)]. From Eq. (14) solving  $p_G = p$  yields only three solutions,  $p_c = 1/2$  and

$$p_{\pm} = \frac{1}{2S} (S \pm (-1 + b)^{\frac{3}{2}} \sqrt{T}), \quad (20)$$

where  $S \equiv -1 + 3b - 3b^2 + b^3$  and  $T \equiv -1 + 3b + b^2 + 5b^3$ . The separators  $p_{c\pm}$  obtained in the preceding subsection do not exist any longer making the phase diagram shown in Fig. 6 very different from the one from Fig. 2. Indeed, it is more like what is expected for the two-dimensional nearest-neighbor ferromagnetic Ising model with a single order-disorder transition.

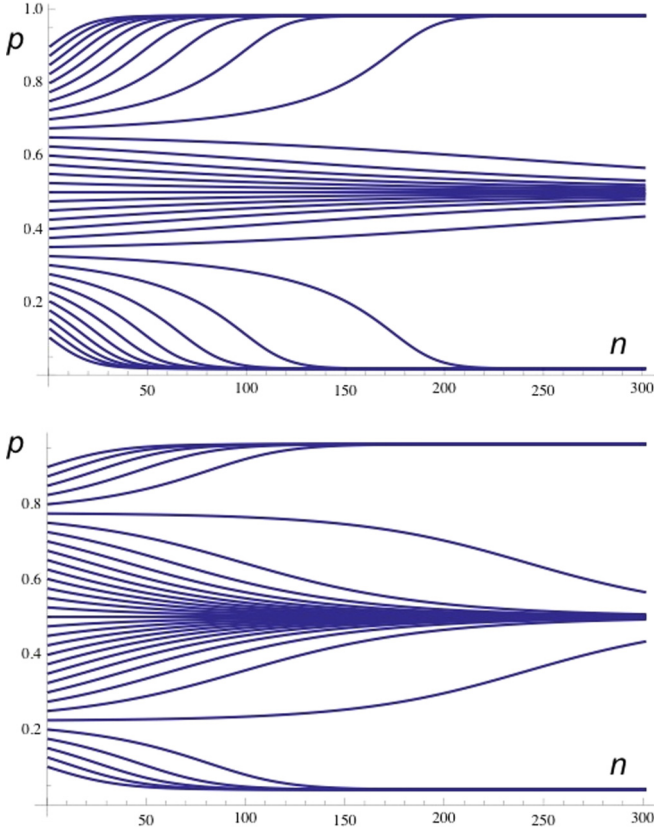


FIG. 5. (Color online) Variation of  $p$  under 30 successive iterations of update rule  $p_G$  using Eq. (12) for  $p_0 = 0.10 + n 0.025$  with  $n = 0, 1, 2, \dots, 32$  at  $b = 0.10$  (upper part) and  $b = 0.13$  (lower part). Both cases satisfy  $b_{c1} < 0.10, 0.13 < b_{c2}$  and show that at the same fixed temperature, depending on the initial condition, i.e., the value of  $p_0$ , the dynamics leads to either the same nonzero value of the magnetization or zero magnetization, which is in total contradiction to what is expected for the second-order Ising transition as exhibited in Fig. 4. The number of iterations are labeled along the abscise.

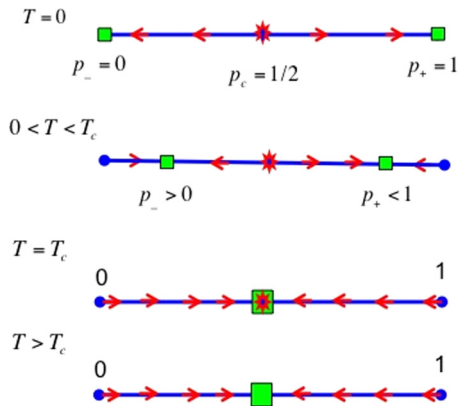


FIG. 6. (Color online) Landscape of the attractors and separators as a function of temperature. The top corresponds to  $T = 0$  with two attractors  $p_-=0$ ,  $p_+=1$  and a separator  $p_c = 1/2$ . Second from top corresponds to  $0 \leq T < T_c \approx 3.09$ : same as before with  $p_- \geq 0$  and  $p_+ \leq 1$ . Third from top: at  $T = T_c$ ,  $p_-$  and  $p_+$  merge with the separator  $p_c$ , which in turn becomes an attractor. Bottom: only one attractor at  $p_c = 1/2$  for  $T > T_c$ .

The associated critical temperature is obtained when  $p_+ = p_- = p_c = 1/2$  yielding  $b_c \approx 0.274$ , which gives  $T_c \approx 3.09$ , whose value is in between the mean-field result  $T_c = 4$  and the exact result  $T_c \approx 2.27$ .

Interestingly, this result is identical to an approximation obtained by Mamada and Tamako [7]. Using a mean-field treatment, the authors calculate a self-consistent equation for the magnetization  $\langle \sigma_i \rangle$ , adding an average over the distribution of the field exerted by the four nearest neighbors on the central single spin. The distribution is thus determined by the possible configurations obtained with four spins ( $\sigma_i = \pm 1$ ). For each one, the associated density matrix  $\rho(\sigma_i = \pm 1)$  reduces to the probability of having  $\pm 1$  with  $\rho(\sigma_i = +1) = p$  and  $\rho(\sigma_i = -1) = (1 - p)$ . From  $\langle \sigma_i \rangle = 2p - 1$  their self-consistent equation [7] rewrites

$$p = \frac{(-2p^3 + 3p^2)(1 - b)^3 - 4pb(b - 1) + b^2(1 + b)}{(1 + b)(1 + b^2)}. \quad (21)$$

On the above basis, Mamada and Tamako calculate the associated dynamics using Glauber and recover the same critical temperature as obtained from Eq. (21).

It is worth noting that Eq. (21) is a self-content equation  $p = f(p)$ , while Eq. (14) is a dynamical equation  $p_G \equiv p(t + 1) = g\{p(t)\}$ . Comparing the right-hand side of both equations shows that they differ only from the coefficient of  $p$  and a division by 5 for the latter. And it happens that

$$\begin{aligned} & -4b(b - 1)p - (1 + b)(1 + b^2)p \\ & = 4(1 + 2b + b^3)p - 5(1 + b)(1 + b^2)p, \end{aligned} \quad (22)$$

which explains why both approaches yields the same fixed points.

At this point GUF combined to Glauber becomes quasi-identical to the Mamada and Tamako approach but turns very different when combined with Metropolis. This puzzling fact has yet to find an explanation.

### C. GUF-Glauber-Onsager-MF

To compare the results obtained with, respectively, Metropolis and Glauber, associated attractor and separator curves are exhibited in Fig. 7 as a function of temperature via the variable  $b$  in abscise together with the Onsager exact solution for the magnetization [31],

$$m_O = (1 - \sinh(2/T)^{-4})^{\frac{1}{8}}, \quad (23)$$

where  $2/T = -1/(2 \ln b)$  and the mean-field formula

$$m_{MF} = \tanh\left(\frac{4m_{MF}}{T}\right), \quad (24)$$

using  $p = (m + 1)/2$  with M, G, O, MF, denoting, respectively, Metropolis, Glauber, Onsager, and mean field. Five critical values  $b_c$  are obtained with labels (1, 2) for Metropolis, label (3) for Onsager, label (4) for Glauber, and label (5) for mean field.

From Fig. 7 it is worth to notice that Metropolis yields a first-order like transition with two critical temperatures  $b_{c1} \approx 0.081$  and  $b_{c2} \approx 0.150$ . However, some discrepancies with a regular first-order transition exist since here. Accordingly,

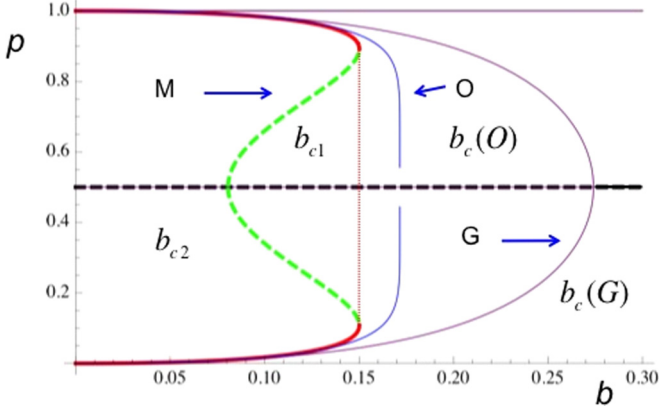


FIG. 7. (Color online) Landscape of the attractors and separators for  $p$  as a function of temperature via the variable  $b = \exp(-4/T)$  in the abscise with Metropolis (M), Glauber (G), Onsager (O), and mean field (MF). Solid lines represent attractors while dashed lines are separators. However, the line  $p_c = 1/2$  is a separator for M, G, O, and MF only when  $b < b_{c1}$  (1). For  $b_{c1}(1) < b < b_{c2}(2)$ ,  $p_c$  is an attractor for M and a separator for O, G, and MF. However, for M other attractors coexist. When  $b_{c2}(2) < b < b_{c3}(3)$ ,  $p_c$  is the unique attractor for M and still a separator for O, G, and MF. For  $b_c(3) < b < b_c(4)$ ,  $p_c$  is an attractor for M, O, but still a separator for G, MF. When  $b_c(4) < b < b_c(5)$ ,  $p_c$  is an attractor for M, O, G, but still a separator for MF. Only when  $b > b_c(5)$ ,  $p_c = 1/2$  is the unique attractor for M, O, G, and MF. We have  $b_{c1} \approx 0.081$ ,  $b_{c2} \approx 0.150$ ,  $b_c(3) \approx 0.171$ ,  $b_c(4) \approx 0.274$ ,  $b_c(5) \approx 0.368$  yielding, respectively,  $T_{c1} \approx 1.59$ ,  $T_{c2} \approx 2.11$ ,  $T_c(3) \approx 2.27$ ,  $T_c(4) \approx 3.09$ ,  $T_c(5) = 4$ .

we do not use the Maxwell construction since GUF does not involve the energy. Therefore, we cannot state that we have a first-order transition but only that the various attractors obey a first-order-like transition.

Moreover, while for a first-order transition, within the range of metastability, the system has a nonzero probability to get trapped into the metastable state as well as the complementary probability to get into the absolute minimum, here given the initial condition, i.e., the value of  $p_0$ , the system reaches either the ordered or the disordered phase with certainty. Given a fixed temperature, within some fixed range of temperature, although two attractors exist, they do not coexist. The outcome is not probabilistic. Each attractor has a well-defined basin of attraction depending on the value  $p_0$  between 0 and 1 as shown in Figs. 3 and 4.

It turns out that critical temperature  $b_{c2} \approx 0.150$  is close to Onsager exact result  $b_c(3) \approx 0.171$ , in addition to exhibit a vertical jump to the disorder phase at  $b_{c2}$ , reminiscent of the rather abrupt vanishing of the corresponding Onsager second-order transition. On the other hand, Glauber is more like MF with an improvement in the value of the critical temperature at  $b_c(4) \approx 0.274$  instead of  $b_c(5) \approx 0.368$  for mean field.

Solid lines represent attractors while dashed lines are separators. However, the line  $p_c = 1/2$  is a separator for M, G, O, and MF only when  $b < b_{c1}$  (1). For  $b_{c1}(1) < b < b_{c2}(2)$ ,  $p_c$  is an attractor for M and a separator for O, G, and MF. But for M other attractors coexist. When  $b_{c2}(2) < b < b_c(3)$ ,  $p_c$  is the unique attractor for M and still a separator for O, G, and MF. For  $b_c(3) < b < b_c(4)$ ,  $p_c$  is an attractor for M, O, but still

a separator for G, MF. When  $b_c(4) < b < b_c(5)$ ,  $p_c$  is an attractor for M, O, G, but still a separator for MF. Only when  $b > b_c(5)$ ,  $p_c = 1/2$  is the unique attractor for M, O, G, and MF. We have  $b_{c1} \approx 0.081$ ,  $b_{c2} \approx 0.150$ ,  $b_c(3) \approx 0.171$ ,  $b_c(4) \approx 0.274$ ,  $b_c(5) \approx 0.368$  yielding, respectively,  $T_{c1} \approx 1.59$ ,  $T_{c2} \approx 2.11$ ,  $T_c(3) \approx 2.27$ ,  $T_c(4) \approx 3.09$ ,  $T_c(5) = 4$ .

## V. DISCUSSION

A coherent and complete picture about the effect of various approximations on departing from the exact treatment of the 2D Ising model is shown in Fig. 7 with, respectively, GUF-Metropolis, GUF-Glauber, Onsager, and mean field.

Metropolis leads to an unexpected intermediate “dis/order” regime between the ordered and disordered phases, turning first-order like the associated transition. It happens that the corresponding critical temperature  $T_{c2} \approx 2.11$  is rather accurate with respect to the exact Onsager value  $T_c \approx 2.27$ . In addition, the transition exhibits a vertical jump to the disorder phase reminiscent of the rather abrupt vanishing of the corresponding Onsager second-order transition. Accordingly, although the “dis/order” regime produced by the GUF-Metropolis combination is not physical, it is an intriguing result worth understanding.

In contrast, combining Glauber dynamics to GUF restores the usual mean-field-like Ising single transition at  $T_c \approx 3.09$ , which asks the question as to why Glauber and Metropolis dynamics lead to different equilibrium states when combined with GUF in the case of the 2D Ising model.

Therefore, GUF needs more investigation to understand its nature and find the origin of those discrepancies with both the classical mean field and the exact result. The question has been evoked in a series of works [16,30,32–34]. One promising direction is to extend the cluster size to which GUF has been applied. Instead of a cluster of five spins limited to the nearest neighbors, it should be interesting to consider both the inclusion of next-nearest neighbors with a nine-spin cluster and also the extension to 3D with a seven-spin cluster, noticing that the respective topologies are instrumental in the calculation of the various GUF coefficients.

Detailed balance is a general principle for systems in thermodynamic equilibrium within Boltzmann statistics. Both Metropolis and Glauber update rules obey detailed balance and yield the equilibrium state when implemented in Monte Carlo simulations. However, when these updated rules are applied with GUF our results show that there exists no guarantee to reach the equilibrium state.

At this stage, the puzzle is twofold: why GUF-metropolis yields an intermediate nonphysical regime and why Metropolis and Glauber combined with GUF yield different physics for the same system while both update schemes are not supposed to produce different physical results?

## ACKNOWLEDGMENTS

We thank Pierre Pfeuty for stimulating critical comments on the manuscript and Dietrich Stauffer for a careful reading of the initial version.

- [1] K. Binder, in *Encyclopedia of Mathematics*, edited by Michiel Hazewinkel (Springer, Berlin, 2001).
- [2] W. Lenz, *Phys. Zeit.* **21**, 613 (1920); E. Ising, *Z. Phys.* **31**, 253 (1925).
- [3] L. Onsager, *Phys. Rev.* **65**, 117 (1944).
- [4] S. Galam, *Europhys. Lett.* **70**, 705 (2005).
- [5] N. Metropolis, A. W. Rosenbluth, M. N. Rosenbluth, A. H. Teller, and E. Teller, *J. Chem. Phys.* **21**, 1087 (1953).
- [6] R. J. Glauber, *J. Math. Phys.* **4**, 294 (1963).
- [7] H. Mamada and F. Takano, *J. Phys. Soc. Japan* **25**, 675 (1968).
- [8] S. Galam, *Sociophysics: A Physicist's Modeling of Psychopolitical Phenomena* (Springer, Berlin, 2012).
- [9] S. Galam, Y. Gefen, and Y. Shapir, *J. Math. Sociol.* **9**, 1 (1982).
- [10] S. Galam and S. Moscovici, *Eur. J. Soc. Psychol.* **21**, 49 (1991).
- [11] K. Sznajd-Weron and J. Sznajd, *Int. J. Mod. Phys. C* **11**, 1157 (2000).
- [12] D. Stauffer, *AIP Conf. Proc.* **690**, 147 (2003).
- [13] A. C. R. Martins, *Int. J. Mod. Phys. C* **19**, 617 (2008).
- [14] C. Castellano, S. Fortunato, and C. Vittorio Loreto, *Rev. Mod. Phys.* **81**, 591 (2009).
- [15] D. Stauffer, *Int. J. Mod. Phys. C* **13**, 975 (2002).
- [16] F. Slanina, K. Sznajd-Weron, and P. Przybyla, *Europhys. Lett.* **82**, 18006 (2008).
- [17] R. Toral and C. J. Tessone, *Commun. Comput. Phys.* **2**, 177 (2007).
- [18] K. Kułakowski and M. Nawojczyk, *Int. J. Mod. Phys. C* **19**, 611 (2008).
- [19] F. Ding, Y. Liu, B. Shen, and X.-M. Si, *Physica A* **389**, 1745 (2010).
- [20] A. C. R. Martins, *AIP Conf. Proc.* **1490**, 212 (2012).
- [21] S. Galam, B. Chopard, A. Masselot, and M. Droz, *Eur. Phys. J. B* **4**, 529 (1998).
- [22] R. Ochrombel, *Int. J. Mod. Phys. C* **12**, 1091 (2001).
- [23] D. Stauffer, *J. Artif. Soc. Soc. Simul.* **5**, 4 (2002).
- [24] P. L. Krapivsky and S. Redner, *Phys. Rev. Lett.* **90**, 238701 (2003).
- [25] M. Mobilia and S. Redner, *Phys. Rev. E* **68**, 046106 (2003).
- [26] L. Behera and F. Schweitzer, *Int. J. Mod. Phys. C* **14**, 1331 (2003).
- [27] F. Slanina and H. Lavicka, *Eur. Phys. J. B*, **35**, 279 (2003).
- [28] J. R. Sanchez, *arXiv:cond-mat/0408518* (2004).
- [29] S. Galam, *Qual. Quant.* **41**, 579 (2007).
- [30] A. O. Souza, K. Malarz, and S. Galam, *Int. J. Mod. Phys. C* **16**, 1507 (2005).
- [31] C. N. Yang, *Phys. Rev.* **85**, 808 (1952).
- [32] R. Lambiotte and S. Redner, *Europhys. Lett.* **82**, 18007 (2008).
- [33] S. Galam and A. C. R. Martins, *Europhys. Lett.* **95**, 48005 (2011).
- [34] P. Przybyla, K. Sznajd-Weron, and M. Tabiszewski, *Phys. Rev. E* **84**, 031117 (2011).